Theoretical Tire Equations for Shimmy and Other Dynamic Studies

LYNN C. ROGERS*
Air Force Flight Dynamics Laboratory, Wright-Patterson Air Force Base, Ohio

Equations are developed which relate ground force and torque on the tire to arbitrary swivel angle and lateral displacement of the wheel rim plane. The theory postulates the string model for the tire since it has predicted behavior substantiated in many respects by experimental results. Approximations to the string model itself are made such that the development leads to linear, constant coefficient differential equations identical in form to an empirical set obtained in an earlier paper. Theoretical frequency responses compare favorably with experimental data.

Nomenclature

a = half contact length
a^* = equivalent half contact length
b = empirical tire parameter
c = constant
F = tire side force
G = transfer or frequency response function
k = distributed elasticity constant
K_F = side force coefficient
K_M = torque coefficient
L = length of tire equator not in contact
M = tire torque
P = distributed side loading
Q = denominator of transfer function
R = see Eq. (17)
r = factor to adjust contact line to equivalent slope
s = Laplace variable
V_x = forward speed
x = prevailing forward motion independent coordinate
y = lateral displacement of axle
z = lateral distortion of tire tread equator from wheel rim plane
z_1 = lateral distortion at contact front
z_0 = lateral distortion at contact center
z_2 = lateral distortion at contact rear
γ = angle, see Fig. 1
ε = see Eq. (24)
η = displacement of tire tread equator from x axis
η_1 = displacement at contact front
η_0 = displacement at contact center
η_2 = displacement at contact rear
λ = wavelength of ground track
ξ = tire equator coordinate
σ = tire relaxation length
τ = string tension
ψ = swivel angle
ω = reduced or path angular frequency
ω_{1-7} = empirical tire parameters
$\overline{(\,)}$ = Laplace transform

Introduction

EQUATIONS relating ground force and torque on the pneumatic tire to arbitrary swivel angle and lateral displacement of the wheel rim plane are required in various dynamic studies. Those studies are concerned with stability and control of vehicle and wheel systems, including shimmy of aircraft landing gears and automotive steering systems. The needed equations which represent the tire accurately and conveniently are provided by the empirical frequency response synthesis method.[1] There are four frequency responses of interest here: a) torque due to swivel angle, b) lateral force due to swivel angle, c) torque due to pure sideslip, and d) lateral force due to pure sideslip. Experimental frequency response data exist for only the first two, and the method must rely on theoretical results for the last two. With regard to the present state-of-the-art, cornering tire theory is of value in two areas: 1) filling the gap where experimental data is not available and 2) placing the empirical synthesized equations on some direct relationship to the physics of the rolling tire. It is to the second area that this paper is addressed.

The theoretical tire models on which investigations have been based may be categorized as the stretched supported string, the stretched supported beam, the extended Moreland model,[1,2] and the Pacejka model.[3] The status of the implementation of extended Moreland theory and of string theory is presented by Collins;[4] there are objections[1] related to the physics of the basic Moreland model and its qualitative agreement with experimental frequency response curves. Pacejka's theory[3] is too cumbersome for direct use in dynamic studies.

The present simplified theory leans heavily on experimental data[5] and the form of the expressions resulting from the empirical method. The theory uses the same string model of the tire as did Segel.[6] Segel's results are striking in that frequency response predictions founded on the string model of the tire correspond well in most respects to experimental observations. Because their form is inconvenient and because certain crucial aspects of the predicted frequency responses are inaccurate, Segel's results are unsuitable for widespread use in dynamics studies. Since the string model represents merely a credible approximation to the intricate physics of the rolling tire, approximations to the string model itself are in order for the purpose of developing a theory which correlated with experimental observations. It is felt that the present development offers physical insight and guidance for further work.

Basic String Model

Referring to Fig. 1, the tire is represented by a string at the tire's equator which is labeled as A102B. The material in this section is adapted from Segel[6] and is included here for completeness. The equation for the elastically supported string under tension is

$$-\tau\partial^2 z(x,\xi)/\partial\xi^2 + kz(x,\xi) = P(x,\xi) \qquad (1)$$

where z is the displacement from the wheel plane, τ is the tension, k is the distributed elasticity constant, and P is the distributed side loading. The homogeneous solution of

Received September 3, 1971; revision received May 3, 1972.
Index categories: Aircraft Landing Dynamics; Structural Stability Analysis.

* Aerospace Engineer, Advanced Metallic Structures Development Program Office, Structures Division (AFFDL/FB-1).

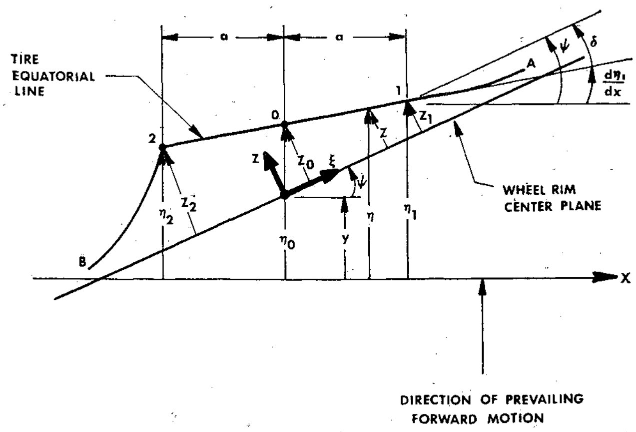

Fig. 1 Geometric relations for the string model of a rolling tire.

Eq. (1) may be written in terms of either exponential or hyperbolic trigonometric functions. The solution in the region of no side loading is written

$$z = c_1' e^{-\xi/\sigma} + c_2' e^{\xi/\sigma}$$

which may be rewritten for later convenience

$$z = c_1 e^{(a-\xi)/\sigma} + c_2 e^{(\xi - a - L)/\sigma}$$

where $\pm 1/\sigma$ are the roots of the characteristic equation. The relaxation length σ is equal to $(\tau/k)^{1/2}$ and the tire equator circumference is $(L + 2a)$, where $2a$ is the length of the contact area. Substitution of the boundary conditions $z = z_1$ at $\xi = a$, and $z = z_2$ at $\xi = a + L$ yields

$$z = z_1 e^{(a-\xi)/\sigma} + z_2 e^{(\xi - a - L)/\sigma}$$

which leads to

$$\partial z(x,\xi)/\partial\xi|_{\xi=a} = -z_1(x)/\sigma; \ \partial z(x,\xi)/\partial\xi|_{\xi=a+L} = z_2(x)/\sigma \tag{2}$$

where

$$z_1(x) = z(x,a); \ z_2(x) - z(x,-a) = z(x,a+L) \tag{3}$$

provided the term $e^{-L/\sigma}$ $(\simeq e^{-6})$ is taken as zero.

The classic assumption of slope continuity is made at point 1, the foremost point of the contact region, which is also the boundary between regions of side loading and no side loading on the string. The assumption is, in effect, that as the tire rolls an infinitesimal amount forward, the infinitesimal arc length on the equator immediately ahead of the contact rolls onto its projection on the ground, which is then part of the contact. Thus, the equatorial line immediately in front of the contact is tangent to the equatorial line just inside the contact. Summing the angles at point 1 gives the geometrical relation

$$d\eta_1(x)/dx + \gamma = \psi(x) \tag{4}$$

Also from Fig. 1,

$$\partial z(x,\xi)/\partial\xi|_{\xi=a} = \tan(2\pi - \gamma) \simeq -\gamma \tag{5}$$

and Eq. (4) becomes

$$d\eta_1(x)/dx - \partial z(x,\xi)/\partial\xi|_{\xi=a} = \psi(x) \tag{6}$$

Another geometrical relation is

$$\eta(x,\xi) = z(x,\xi) + y(x) + \xi\psi(x) \tag{7}$$

or

$$\bar{\eta}(s,\xi) = \bar{z}(s,\xi) + \bar{y}(s) + \xi\bar{\psi}(s) \tag{8}$$

where the bar indicates the Laplace Transform, and s is the Laplace variable. The operational notation is used for convenience in manipulating the differential equations and initial conditions are not required. At point 1, Eq. (7) becomes

$$\eta_1(x) = z_1(x) + y(x) + a\psi(x) \tag{9}$$

or

$$\bar{\eta}_1(s) = \bar{z}_1(s) + \bar{y}(s) + a\bar{\psi}(s) \tag{10}$$

Combining Eqs. (2, 6 and 9) results in the fundamental equation

$$\sigma d\eta_1(x)/dx + \eta_1(x) = (\sigma + a)\psi(x) + y(x) \tag{11}$$

or

$$(\sigma s + 1)\bar{\eta}_1(s) = (\sigma + a)\bar{\psi}(s) + \bar{y}(s) \tag{12}$$

The classic assumption of adhesion is made for the region 102 and leads to

$$\eta(x,\xi) = \eta_0(x + \xi); \ -a \leq \xi \leq a \tag{13}$$

or

$$\bar{\eta}(s,\xi) = e^{\xi' s}\bar{\eta}_0(s); \ \xi' = \xi - a \tag{14}$$

Approximation to the String Model

Expanding the equator displacement from the line of prevailing forward motion into a power series eventually results in linear, constant coefficient differential equations. The Taylor series for Eq. (13) is

$$\eta(x,\xi) = \eta_0(x) + \xi d\eta_0(x)/dx + (\xi^2/2)d^2\eta_0(x)/dx^2 + \cdots \tag{15}$$

or

$$\bar{\eta}(s,\xi) = (1 + \xi s + \xi^2 s^2/2 + \cdots)\bar{\eta}_0(s) \tag{16}$$

which may be written

$$\bar{\eta}(s,\xi) = [1 + \xi s + sR(\xi,s)]\bar{\eta}_0(s) \tag{17}$$

where the polynomial R is defined implicitly.

Because of the adhesion assumption, the path of the equator on the ground is a curve. In the wavelength range of interest, the segment of the curve in contact region 102 is suitably represented by the straight line

$$\eta(x,\xi) = \eta_0(x) + r\xi d\eta_0(x)/dx \tag{18}$$

or

$$\bar{\eta}(s,\xi) = (1 + r\xi s)\bar{\eta}_0(s) \tag{19}$$

At point 1, Eq. (19) may be evaluated

$$\eta_1(x) = \eta(x,a) = \eta_0(x) + ra^* d\eta_0(x)/dx \tag{20}$$

or

$$\bar{\eta}_1(s) = (1 + ra^* s)\bar{\eta}_0(s) \tag{21}$$

where the factors

$$r \simeq 1 \qquad a^* \simeq a \tag{22}$$

have been introduced to trace the origin of terms in subsequent equations and to aid in the discussion. [Note the correspondence between Eq. (18) and Smiley's[7] C2 approximation.]

Eliminating $\bar{\eta}$, $\bar{\eta}_1$ and $\bar{\eta}_0$ from Eqs. (8, 12, 19 and 21) and solving for $\bar{z}$ gives

$$\bar{z}(s,\xi) = \{[(\sigma + a - \xi) + \xi(r\sigma + ra - \sigma - ra^*)s - \xi ra^*\sigma s^2]\bar{\psi}(s) - [(\sigma + ra^* - r\xi) + ra^*\sigma s]s\bar{y}(s)\}/(\sigma s + 1)(1 + ra^* s) \tag{23}$$

Let the coefficient of $s\psi$ be represented

$$\xi\varepsilon = \xi[\sigma(1 - r) + r(a^* - a)] \tag{24}$$

The actual path of the equator on the ground will deviate slightly from the straight line Eq. (18) with $r=1$. The r and a^* factors may be considered to represent another straight line, which accounts for the net physical effects. The departure of r and a^* from 1 and a respectively is of secondary importance in Eq. (23) except for the coefficient (24). This coefficient is composed of differences between approximately equal quantities, a notably sensitive situation. Representation of the coefficient by the left hand side of Eq. (24), where ε is a small positive number, leads to frequency responses which agree with experiment.†

Using Eq. (24) as the coefficient of $s\psi$ and Eq. (22) otherwise gives

$$\bar{z}(s,\xi) = \{[(\sigma + a - \xi) + \xi\varepsilon s - \xi a\sigma s^2]\bar{\psi}(s) - [(\sigma + a - \xi) + a\sigma s]s\bar{y}(s)\}/(\sigma s + 1)(1 + as) \quad (25)$$

or more conveniently

$$Q_2(s)\bar{z}(s,\xi) = [(\sigma + a - \xi) + \xi\varepsilon s - \xi a\sigma s^2]\bar{\psi}(s) - [(\sigma + a - \xi) + a\sigma s]s\bar{y}(s) \quad (26)$$

where

$$Q_2(s) = (\sigma s + 1)(1 + as) \quad (27)$$

Note that the order of this polynomial Q is dependent on the truncation Eq. (18). The quantities

$$\bar{z}_1(s) = \bar{z}(s,a);\ \bar{z}_2(s) = \bar{z}(s,-a) \quad (28)$$

will be required.

Force and Moment Integrals

The force of the ground on the tire is given by[6]

$$F(x) = \int_{-a}^{a} P(x,\xi)d\xi \quad (29)$$

Substitution of Eq. (1) and partial evaluation using Eq. (2) results in

$$F(x) = k\int_{-a}^{a} z(x,\xi)d\xi + k\sigma[z_1(x) + z_2(x)] \quad (30)$$

or

$$Q(s)\bar{F}(s) = k\int_{-a}^{a} Q(s)\bar{z}(s,\xi)d\xi + k\sigma[Q(s)\bar{z}_1(s) + Q(s)\bar{z}_2(s)] \quad (31)$$

where Q is not a function of ξ. Similarly, the expression for torque

$$M(x) = -\int_{-a}^{a} \xi P(x,\xi)d\xi \quad (32)$$

leads to

$$M(x) = -k\int_{-a}^{a} z(x,\xi)\xi d\xi - k\sigma(\sigma + a)[z_1(x) - z_2(x)] \quad (33)$$

and

$$Q(s)\bar{M}(s) = -k\int_{-a}^{a} Q(s)\bar{z}(s,\xi)\xi d\xi - k\sigma(\sigma + a)[Q(s)\bar{z}_1(s) - Q(s)\bar{z}_2(s)] \quad (34)$$

† In the context of a simplified theory it does not appear possible to present a completely satisfying heuristic explanation of the ε term, if at all. The final justification is the agreement of the resulting theoretical frequency responses with experimental data. This is discussed further in the Appendix. The more sophisticated theory of Pacejka[3] indicates that the combined effect of longitudinal tread distortion and finite tread width account for the term. The obvious questions of tread bending stiffness, partial sliding of the contact, tire hysterisis, and tread inertia are not addressed in the present effort.

Differential Equations

Evaluation of Eqs. (31) and (34) by use of Eqs. (26) and (28) yields

$$Q_2(s)\bar{F}(s) = K_F\{\bar{\psi}(s) - [1 + a\sigma s/(\sigma + a)]s\bar{y}(s)\} \quad (35)$$

and

$$Q_2(s)\bar{M}(s) = K_M\{[1 + \varepsilon s + a\sigma s^2]\bar{\psi}(s) - s\bar{y}(s)\} \quad (36)$$

where

$$K_F = 2k(\sigma + a)^2 \quad (37)$$

(commonly called cornering power) and

$$K_M = 2ka[a^2/3 + \sigma(\sigma + a)] \quad (38)$$

The two parameters K_F and K_M are used to replace the one parameter k because of relative ease and certainty of experimental determination and lack of confidence in the theoretical relationship. For convenience, define the quantity b by the equation

$$\varepsilon = 2b(a\sigma)^{1/2} \quad (39)$$

Applying the inverse transform to Eqs. (35) and (36), and substituting

$$d/dx = (1/V_x)d/dt \quad (40)$$

gives the corresponding differential equations

$$M + [(a + \sigma)/V_x]\dot{M} + [a\sigma/V_x^2]\ddot{M} = K_M\{\psi + [2b(a\sigma)^{1/2}/V_x]\dot{\psi} + [a\sigma/V_x^2]\ddot{\psi} - [1/V_x]\dot{y}\} \quad (41)$$

$$F + [(a + \sigma)/V_x]\dot{F} + [a\sigma/V_x^2]\ddot{F} = K_F\{\psi - [1/V_x]\dot{y} - [a\sigma/(a + \sigma)V_x^2]\ddot{y}\} \quad (42)$$

The equations established empirically[1] are

$$M + [1/\omega_1 + 1/\omega_3](1/V_x)\dot{M} + [1/\omega_1\omega_2 V_x^2]\ddot{M} = K_M\{\psi + [2b_1/\omega_2 V_x]\dot{\psi} + [1/\omega_2^2 V_x^2]\ddot{\psi} - [1/V_x]\dot{y}\} \quad (43)$$

$$F + [2b_2/\omega_4 V_x]\dot{F} + [1/\omega_4^2 V_x^2]\ddot{F} = K_F\{\psi - [1/V_x]\dot{y} - [1/\omega_7 V_x^2]\ddot{y}\} \quad (44)$$

Equations (41) and (42) are identical in form to Eqs. (43) and (44).

Comparison of Frequency Responses

The transfer function from Eq. (35) relating $\bar{M}$ to $\bar{\psi}$ for pure yaw is

$$G_{M\xi}{}^t(s) = \bar{M}(s)/\bar{\psi}(s) = K_M[1 + 2b(a\sigma)^{1/2}s + a\sigma s^2]/(\sigma s + 1)(1 + as) \quad (45)$$

and the frequency response is obtained by substituting $j\omega$ (where ω is the reduced angular frequency) for s

$$G_{M\psi}{}^t(j\omega) = K_M[1 + 2b(a\sigma)^{1/2}j\omega + a\sigma(j\omega)^2]/(\sigma j\omega + 1)(1 + aj\omega) \quad (46a)$$

Similarly, the remaining theoretical frequency responses are

$$G_{F\psi}{}^t(j\omega) = K_F/(\sigma j\omega + 1)(1 + aj\omega) \quad (46b)$$

$$G_{M\dot{y}}(j\omega) = K_M/(\sigma j\omega + 1)(1 + aj\omega) \quad (46c)$$

$$G_{F\dot{y}}{}^t(j\omega) = K_F[1 + a\sigma j\omega/(a + \sigma)]/(\sigma j\omega + 1)(1 + aj\omega) \quad (46d)$$

The corresponding synthesized frequency responses are obtained from Eqs. (43) and (44)

$$G_{M\psi}{}^s(j\omega) = K_M[1 + 2b_1 j\omega/\omega_2 + (j\omega/\omega_2)^2]/[1 + (1/\omega_1 + 1/\omega_3)j\omega + (j\omega)^2/\omega_1\omega_3] \quad (47a)$$

$$G_{F\psi}{}^s(j\omega) = K_F/[1 + 2b_2 j\omega/\omega_4 + (j\omega/\omega_4)^2] \quad (47b)$$

$$G_{M\dot{y}}{}^s(j\omega) = K_M/[1 + (1/\omega_1 + 1/\omega_3)j\omega + (j\omega)^2/\omega_1\omega_3] \quad (47c)$$

$$G_{F\dot{y}}{}^s(j\omega = K_F[1 + j\omega/\omega_7]/[1 + 2b_2 j\omega/\omega_4 + (j\omega/\omega_4)^2] \quad (47d)$$

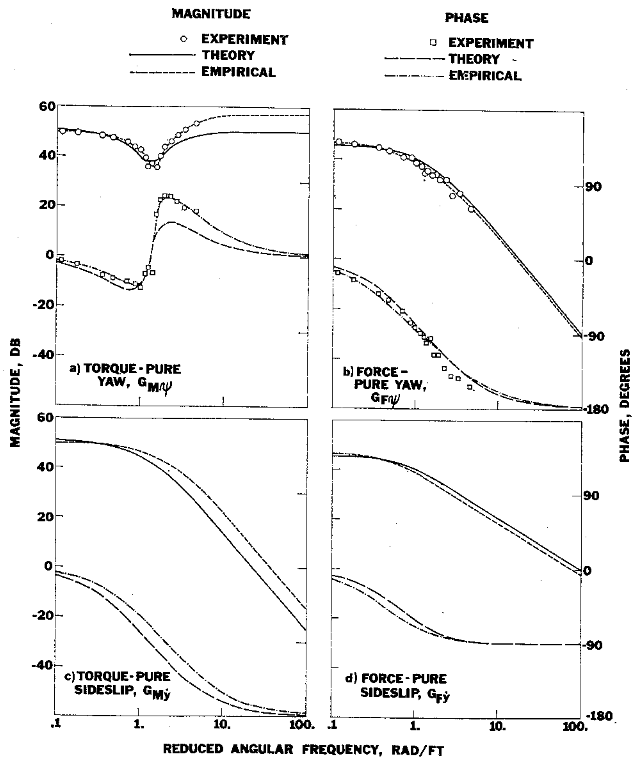

Fig. 2 Comparison of frequency response curves and experimental data.

The theoretical parameters K_F, K_M, a, σ and b were determined for the same experimental frequency response data used in Ref. (1). A least squares procedure used the distances in the complex plane from the experimental points to the theoretical curve at the same frequency. The unweighted sum of squares was extended over both force and torque simultaneously.

The resulting theoretical curves Eqs. (46) are compared to the experimental data and to the synthesized curves Eqs. (47) in Fig. 2. For sinusoidal motion the wavelength λ of the equatorial ground track is related to the reduced angular frequency by the equation

$$\lambda = 2\pi/\omega \tag{48}$$

The ratio

$$2a/\lambda = a\omega/\pi \tag{49}$$

is the fraction of a complete sinusoidal wavelength that the straight line segment Eq. (18) represents. For $a = 0.404$ and $2a/\lambda = 0.25$, it follows that $\omega = 1.94$, which would certainly be an upper limit. Because of this consideration, the high frequency experimental points were discarded one by one until the resulting value for the half footprint length a and the highest experimental frequency used were compatible. A comparison of the curves in Fig. 2 demonstrates excellent qualitative agreement and reasonable quantitative agreement for such a grossly simplified theory.

Discussion

Based on the comparison of the experimental data and the theoretical curves in Fig. 2, it must be concluded that the theory provides an engineering approximation to the behavior of the tire. The usefulness of the theory does not lie in using Eqs. (41) and (42) in dynamics studies. At present the appropriate theoretical parameter values can only be determined with confidence from experimental frequency response data. Given that data, the empirical parameter values in Eqs. (43) and (44) can also be determined, and yield a better representation of the tire. The usefulness of the theory lies in the physical insight it gives and in its potential to utilize more sophisticated theory and/or more simplified experiment. The theory also offers the possiblity of performing a sensitivity analysis of dynamic study results to the parameters and perhaps tailoring the tire construction to particular desired characteristics.

It should be noted that the correlation between the values for the half tread length a determined from the experimental frequency response and from measurement of the contact length is unknown. The same situation exists for the relaxation length σ for which Smiley and Horne[8] give four experimental procedures.

As was emphasized in the introduction, the development was substantially guided by the desired results. The underlying philosopy is that it is inappropriate from a practical engineering viewpoint to adopt a grossly simplified model and then to avoid approximations and simplifications to the model itself, especially when they are necessary in the interest of correlating with experiment, or when convenience results without sacrificing accuracy. The particular steps motivated in this way were 1) using the series representation for η, 2) truncating the series at two terms, and 3) retaining the ε term. The background for this theory includes fitting of frequency response curves with ratios of polynomials, and the series representation leads to corresponding polynomials, and then to linear constant coefficient differential equations. This type is preferable in theoretical studies. Truncating the series at two terms results in second order polynomials and differential equations consistent with Eqs. (43) and (44). Retaining the ε term leads to a correct representation of the net physical effects in torque due to swivel angle.

The theoretical equations are identical in form to those developed empirically in Ref. 1, i.e., the same coordinate variables and their derivatives occur. The coefficients are in terms of theoretical parameters in the one case, and empirical parameters in the other. There are five theoretical parameters: a, σ, K_F, K_M and b; whereas there are nine empirical tire parameters: ω_1, ω_2, ω_3, b_1, K_M, ω_4, b_2, K_F, and ω_7. Obviously, there is a possibility of contradictory results. At present, however, there is no frequency response data to determine the lateral displacement empirical parameters. Moreover, there is some latitude in determining the empirical parameters from experimental frequency response curves. The net effect is that the situation cannot be conclusively assessed at present. It is again emphasized that the theory must be used with care. It remains for future experimental and theoretical work with tires alone and with typical dynamic systems to establish the total usefulness of the tire theory and the best procedures.

Appendix

It is informative to compare the $\bar{z}$'s in the truncated series form Eq. (25), the exponential form, and the infinite series form. If the exponential form Eq. (14) is used in place of Eq. (19) and the exponential form corresponding to Eq. (21) are used with Eqs. (8) and (12), the resulting expression for $\bar{z}$ is

$$\bar{z}_e(s,\xi) = \{[(\sigma + a)e^{\xi s} - (\sigma s + 1)\xi e^{as}]\bar{\psi}(s) + [e^{\xi s} - (\sigma s + 1)e^{as}]\bar{y}(s)\}/(\sigma s + 1)e^{as} \tag{A1}$$

Segel[6] uses an expression equivalent to this and develops force and torque frequency responses in terms of transcendental functions. Use of Eqs. (8, 12, and 17) and the series expression corresponding to Eq. (21) yields for $\bar{z}$

$$\bar{z}_R(s,\xi) = (\{(\sigma + a - \xi) + [-a\sigma s^2 + (\sigma + a)sR(\xi,s) - sR(a,s) - s^2\sigma R(a,s)]\}\bar{\psi}(s) - \{(\sigma + a - \xi) + a\sigma s + [-R(\xi,s) + R(a,s) + \sigma s R(a,s)]\}s\bar{y}(s))/(\sigma s + 1)[1 + as + sR(a,s)] \tag{A2}$$

Whereas the integrals Eqs. (29) and (32) are used here to develop force and moment expressions, some analysts use linear combinations of z evaluated at discrete points. Regardless of which approach is used, the series representation leads to a frequency response of torque to swivel angle, $G_{M\psi}(j\omega)$, in which the coefficient of the $j\omega$ term in the numerator is zero and higher terms are not zero. This occurs because the coefficient of $s\bar{\psi}$ in Eq. (A2) is zero. When one of the coefficients of a polynomial is zero, there are either pure imaginary roots or roots with positive real parts. The polar plot of $G_{M\psi}(j\omega)$ starts on the positive real axis for ω equal to zero, moves clockwise toward the origin as ω increases, passes near the origin, and continues toward the positive real axis. For a conjugate pair of pure imaginary zeros, the plot passes through the origin; for a conjugate pair of zeros with positive real parts, the plot circles the origin. (Segel's circles the origin.) From physical consideration of phase angles at high frequencies, the plot must not circle the origin.

The approach of $G_{M\psi}(j\omega)$ to the origin is seen to be crucial. The string model is inadequate to yield the correct results on this sensitive point, although it does indicate a close approach to the origin and yields the proper characteristics of the remaining frequency responses. The effect of the ε term in the theory of the paper is to cause $G_{M\psi}\varepsilon(j\omega)$ not to pass through or to circle the origin.

The denominators of Eqs. 23, A1 and A2) roughly correspond to characteristic functions [see Eqs. (31) and (34)]. Comparing Eqs. (A1) and (A2) it is seen that the polynomial approximates the exponential, which has no roots. With this and the above paragraphs in mind, it is not surprising that some shimmy investigators have found that truncations of the series can introduce spurious roots.

References

[1] Rogers, L. C. and Brewer, H. K., "Synthesis of Tire Equations for Shimmy and other Dynamic Studies," *Journal of Aircraft*, Vol. 8, No. 9, Sept. 1971, pp. 689–697

[2] Collins, R. L. and Black, R. J., "Tire Parameters for Landing-Gear Shimmy Studies," *Journal of Aircraft*, Vol. 6, No. 3, May-June 1969, pp. 252–258.

[3] Pacejka, H. B., "The Wheel Shimmy Phenomenon," Ph.D. thesis, 1966, Delft Technical Institute, Delft, Holland.

[4] Collins, R. L., "Theories on the Mechanics of Tires and Their Applications to Shimmy Analysis," *Journal of Aircraft*, Vol. 8, No. 4, April 1971, pp. 271–277.

[5] Brewer, H. K., "Cornering Force and Self-Aligning Torque Response of a Tire Undergoing Sinusoidal Variations in Steer Angle," Rept. Nov. 1965, B. F. Goodrich Research Center, Brecksville, Ohio.

[6] Segel, L., "Force and Moment Response of Pneumatic Tires to Lateral Motion Inputs," *Transactions of the ASME, Journal of Engineering for Industry*, 88B, 1966, 1, 8 p.; also Paper 65-Av-2.

[7] Smiley, R. F., "Correlation, Evaluation, and Extension of Linearized Theories for Tire Motion and Wheel Shimmy," Rept. 1299, 1957, NACA.

[8] Smiley, R. F. and Horne, W. B., "Mechanical Properties of Pneumatic Tires with Special Reference to Modern Aircraft Tires," TR-R-64, 1960, NASA.

AUGUST 1972 J. AIRCRAFT VOL. 9, NO. 8

Combined Viscous-Inviscid Analysis of Supersonic Inlet Flowfields

THEODORE A. REYHNER* AND TIMOTHY E. HICKCOX†
The Boeing Company, Seattle, Wash.

A procedure is described for analytically predicting the flowfield in the supersonic diffuser of a supersonic inlet. It differs from existing techniques which calculate the inviscid flow in the inlet independent of the viscous flow by calculating the effects of the viscous flow on the inviscid flowfield of the inlet. The procedure consists of first calculating the inviscid flow without viscous effects. Then the boundary-layer growth in the inlet including bleed, bleed scoops and shock wave/boundary-layer interactions is calculated. A second inviscid flow calculation is then made which is matched to the boundary-layer solution. The various steps of the procedure are described with emphasis on the matching of the viscous (boundary layer) and inviscid solutions. Comparisons of predictions with experiments for a Mach 3.0 and a Mach 2.65 mixed-compression supersonic inlet show that this procedure accurately predicts the inlet flowfields and that the effects of the boundary layer on the flowfield are very significant.

Nomenclature

$\dot{m}_{BL}$ = bleed mass flow
$\dot{m}_{139}$ = bleed mass flow used for boundary-layer computation
n = coordinate normal to inlet surface
p_p = Pitot probe pressure
p_s = static pressure
R = distance from surface to inlet axis
R_L = radius of inlet lip
u = velocity component parallel to surface
X = coordinate along inlet axis
δ^* = boundary-layer displacement thickness,

$$\int_0^\delta \left(1 - \frac{\rho u}{\rho_e u_e}\right) dn$$

δ^*_{BL} = bleed equivalent displacement thickness, $(\dot{m}_{BL}/\rho_e u_e 2\pi R)$ (axisymmetric inlet)
δ = boundary-layer thickness
η = bleed efficiency parameter
ρ = density

Presented as Paper 72-44 at the AIAA 10th Aerospace Sciences Meeting, San Diego, Calif., January 17–19, 1972; submitted January 27, 1972; revision received May 8, 1972.

Index categories: Subsonic and Supersonic Airbreathing Propulsion; Jets, Wakes and Viscid-Inviscid Flow Interactions.

* Senior Engineer, Commercial Airplane Group. Member AIAA.

† Engineer, Commercial Airplane Group.